Int. J. Electrochem. Sci., 17 **(2022)** Article Number: 220437, doi: 10.20964/2022.04.49

International Journal of
ELECTROCHEMICAL
SCIENCE
www.electrochemsci.org

Erosion-corrosion Behavior of Q235 Carbon Steel in Sand-containing Solutions

Teng Wu[1], *Qihang Hu*[2], *Xuesen Zhang*[3], *Shuai Qu*[4], *Xinguo Feng*[1,*]

[1] College of Harbour, Coastal and Offshore Engineering, Hohai University, Nanjing 210098, Jiangsu, China
[2] Ningbo water conservancy & hydropower planning and design institute CO.,LTD, Ningbo 315000, Zhejiang, China
[3] CGN New Holdings Co.,Ltd., Beijing, 100071, China
[4] AVIC BIAM New Materials Technology & Engineering Co., Ltd, Beijing, 100095, China
[*]E-mail: fengxingguo@hhu.edu.cn

Received: 3 January 2022 / *Accepted:* 11 February 2022 / *Published:* 4 March 2022

The effects of the sand content, rotational speed, and size of sand particles on the erosion-corrosion behavior on Q235 carbon steel have been studied using electrochemical tests and weight loss measurements. The surface topographies of carbon steel samples were observed after 10 h of an erosion-corrosion test. The results suggest that the total weight loss rate of carbon steel was accelerated upon increasing sand content and rotational speed in the sand-containing solution. Simultaneously, the indentations on the carbon steel surface also increased with the rotational speed and sand content in the sand-containing solution. The carbon steel sample in the solution containing the medium-fine sand was seriously eroded when compared to its counterpart in the solution with the same content of coarse sand at a low rotational speed, while the samples in the latter solution were more obviously eroded at a high rotational speed. In addition, the total weight loss rate of carbon steel originated from the pure erosion of the sand particles and the weight loss rate caused by pure corrosion was ~10–20% of the total weight loss rate.

Keywords: Carbon steel, erosion-corrosion behavior, sand-containing solution, surface characterization

1. INTRODUCTION

Steel structures in hydraulic engineering are prone to corrosion because they are located in damp and dark environments in the presence of aquatic organisms for long periods of time [1]. In particular, rivers contain a high content of sediment, which is carried by the water current and repeatedly impacts with the steel structure to cause damage in the form of micro-cutting, ploughing, and impact deformation

[2], aggravating the corrosion damage in the steel structure. Erosion and corrosion damage leads to a decrease in the yield strength and fracture toughness of steel structures used in hydraulic engineering [3], which decreases the stability of the steel structure components [4] and reduces the safety of steel structure in hydraulic engineering.

There are multiple factors that affect the erosion and corrosion behavior of steel structures in hydraulic engineering, among which the sediment characteristics is one of the key factors. The sediment characteristics include the sand concentration, sand particle size, geometric shape, grain size gradation, etc. Paul [5] studied the effect of erosion-corrosion behavior on API X120 steel and P110 steel respectively, and reported that larger sand particles led to more obvious erosion-corrosion damage on the two types of steel studied. However, Gou [6] confirmed that there is a critical value for the sediment particles on the erosion-corrosion behavior of 45 mild steel and the effect of sand particles had a significant influence on the mass loss of the steel when the sand particles are greater than the critical value.

In fact, sediment carried by natural rivers is composed of various particle sizes of sand. In another words, the grain size gradation of sand in natural rivers is complex. For example, in the Yangtze River, large particles comprised of pebbles and gravel are often carried to the upper reaches due to the large terrain difference along the way and high flow velocity [7, 8], while silty-fine sand is carried by the water flow in the middle and downstream sections due to the decrease in the flow velocity [9, 10]. The grain size of sediment is an important index of the sediment carrying capacity of water flow, which indicates the erosion-corrosion ability on the steel structures used in hydraulic engineering.

Previous studies have mainly investigated the erosion-corrosion behavior of single-size particles on various steels and ignored the effect of the grain size gradation of sand on the erosion-corrosion behavior. In the present study, the erosion-corrosion behavior of Q235 carbon steel in solutions containing two kinds of grain size gradation sand were measured using weight loss tests and electrochemical methods, and the surface was observed using SEM. In addition, the influence of the rotational speed and sand content on the erosion-corrosion behavior were also studied.

2. MATERIALS AND EXPERIMENTS

2.1 Materials

Q235 carbon steel, whose chemical composition is listed in Table 1, was prepared with a size of 35 × 25 × 1.5 mm for our experiments. The samples were polished to No. 800 using SiC sandpaper. The carbon steel samples were then degreased and washed using acetone and deionized water, respectively. Copper wire was welded onto the carbon steel samples, which were then coated with silica gel, leaving an area of 2.0 cm^2 for electrochemical testing and mass loss analysis.

Table 1. Chemical composition of Q235 carbon steel (wt.%)

Steel	C	Mn	Si	P	S	Fe
Q235 carbon steel	0.20	0.42	0.21	0.03	0.008	Balance

Two kinds of grain size gradation sand were adopted. One type with a particle size ranging from 0.5 to 1 mm (Fig.1 (a), (b)) and median particle size (D_{50}) of 0.775 mm was classified as coarse sand (named A). The other type was medium-fine sand (named B) and the median particle size D_{50} was 0.270 mm (Fig.1 (c), (d)).

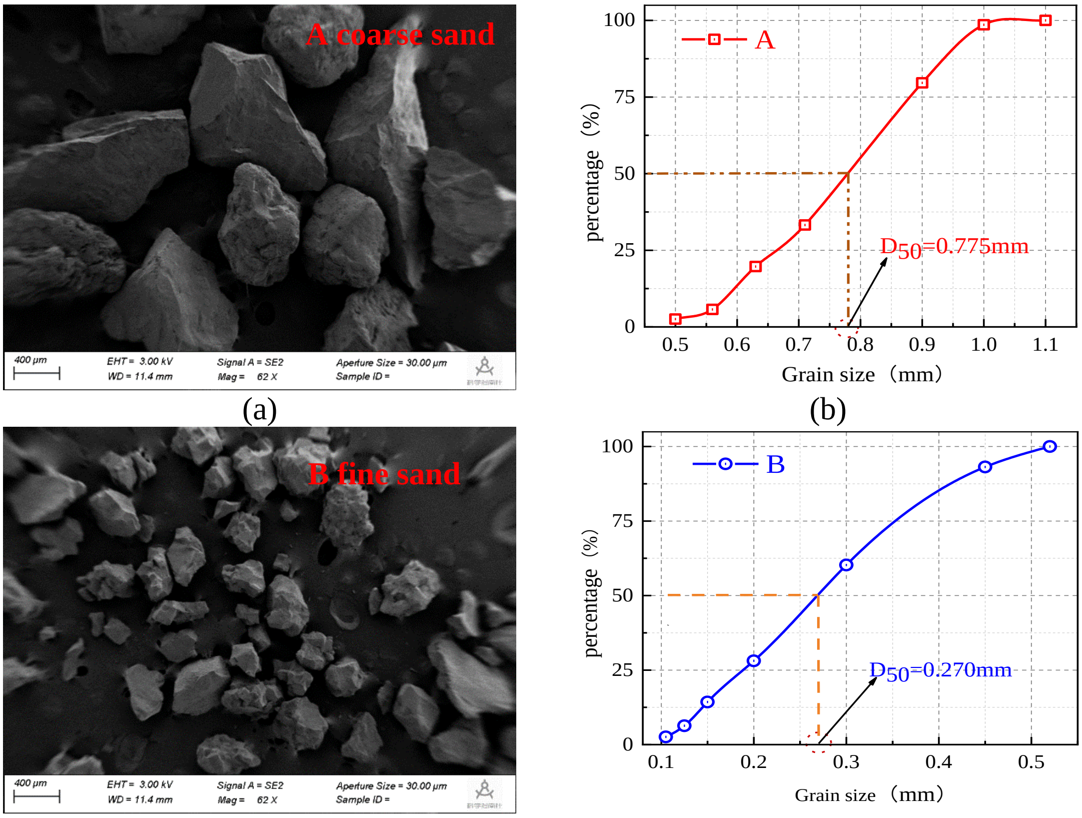

(a) (b)

(c) (d)

Figure 1. The morphology and grain size gradation of the (a, b) coarse (A) and (c, d) medium-fine sand (B) samples.

2.2 Experimental procedure

A home-made device was used to carry out the erosion-corrosion experiment, as shown in Fig. 2. In the device, four blades promote the rotation of the sand-containing solution and the Q235 carbon steel samples were fixed on the inside wall of the cylinder. It is worth mentioning that the rotating shaft and leaf were made from steel covered coated with plastic in the home-made device, which was designed to avoid any interference on the electrochemical measurements. Under each condition, six carbon steel samples were continuously tested for 10 h, in which three samples were assigned for electrochemical measurements, while the remaining three samples were used for weight loss tests. It is worth mentioning that all the experiments were performed at room temperature (20 °C).

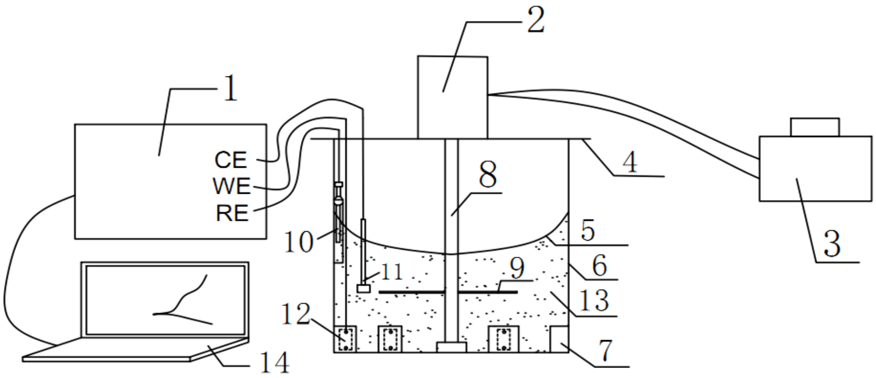

Front view

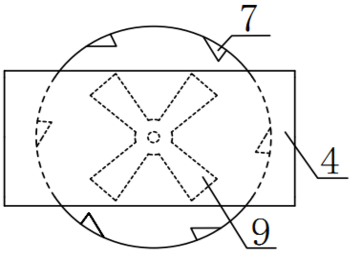

Top view

Figure 2. A schematic diagram of the homemade device used for erosion-corrosion experiments. Note: 1) Electrochemical workstation, 2) motor, 3) voltage regulator, 4) cylinder cover plate, 5) liquid level, 6) device cylinder wall, 7) bottom chute, 8) rotating shaft (steel bars coated with plastic), 9) leaf (steel coated with plastic), 10) reference electrode, 11) auxiliary electrode, 12) sample, 13) sand-laden aqueous solution, 14) computer.

To investigate the erosion-corrosion behavior of Q235 carbon steel, the sand content and rotational speed in the solutions were controlled at 25, 50, and 100 kg/m^3, and 500, 750, and 1000 rpm, respectively. For comparison, the solutions without sand (tap water) at different rotational speeds were designed as the control conditions. The solution conductivity of the tap water was 130 mS/cm, and the conductivity was 118, 103, and 89 mS/cm for the solutions containing 25, 50, and 100 kg/m^3 coarse sand (A). When the solutions contained 25, 50, and 100 kg/m^3 medium-fine sand (B), their conductivity values were 109, 97, and 86 mS/cm, respectively. A total of 21 experimental groups were performed in this study, as shown in Table 2.

Weight loss tests were conducted using an electronic balance with a scale interval of 0.01 mg. The total weight loss rate (w_{total}) of the carbon steel samples in each erosion-corrosion experiment was calculated according to Eq. (1):

$$w_{total} = \frac{m_0 - m_t}{s \cdot t} \qquad (1)$$

where m_0 and m_t represent the weight before and after the erosion-corrosion experiment over t hours and s is the surface area of the carbon steel subjected to erosion-corrosion. Under each condition, three carbon steel samples were used in the weight loss test and the average values reported.

Table 2. Erosion-corrosion experimental conditions.

Test group number	Sand particle size	Speed(rpm)	sand concentration (kg/m^3)	Test group number	Sand particle size	Speed(rpm)	Sand concentration (kg/m^3)
1	Tap water	500rpm	0				
2	0.5-1mm(A)	500rpm	25	13	0.1-0.5mm(B)	500rpm	25
3	0.5-1mm(A)	500rpm	50	14	0.1-0.5mm(B)	500rpm	50
4	0.5-1mm(A)	500rpm	100	15	0.1-0.5mm(B)	500rpm	100
5	Tap water	750rpm	0				
6	0.5-1mm(A)	750rpm	25	16	0.1-0.5mm(B)	750rpm	25
7	0.5-1mm(A)	750rpm	50	17	0.1-0.5mm(B)	750rpm	50
8	0.5-1mm(A)	750rpm	100	18	0.1-0.5mm(B)	750rpm	100
9	Tap water	1000rpm	0				
10	0.5-1mm(A)	1000rpm	25	19	0.1-0.5mm(B)	1000rpm	25
11	0.5-1mm(A)	1000rpm	50	20	0.1-0.5mm(B)	1000rpm	50
12	0.5-1mm(A)	1000rpm	100	21	0.1-0.5mm(B)	1000rpm	100

A CS310H workstation (Corrtest, China) was used to conduct the electrochemical tests, including the open circuit potential (OCP), electrochemical impedance spectroscopy (EIS), and potentiodynamic polarization curves. A three electrode system was used in these electrochemical measurements. The Q235 carbon steel sample, a saturated calomel electrode, and platinum sheet electrode were used as the working, reference and counter electrodes, respectively. After 8 h of the erosion-corrosion test, the OCP value of the sample was tested. EIS measurements were conducted with a disturbance amplitude of 10 mV in the range from 10^5 to 10^{-2} Hz after 9 h. Finally, because the erosion-corrosion test was carried out for 10 h, the potentiodynamic polarization curves of the carbon steel samples were obtained to determine the pure erosion current density from –0.3 to 1.2 V vs OCP at a scan rate of 0.5 mV/S under a potential of –0.9 V_{SCE} to ensure full cathodic protection [10]. In addition, the surfaces of the Q235 carbon steels were observed using a Zeiss Sigma 300 scanning electron microscope after 10 hours of the erosion-corrosion test.

3. RESULTS AND DISCUSSION

3.1 Open circuit potential

Fig. 5 shows the OCP values of the carbon steel samples were in the range of –0.4 to -0.3 V_{SCE} and the values were negatively shifted upon increasing the sand content [11]. The OCP of the sample in the solution containing coarse sand (A) was obviously lower than that of the one in the solution containing medium-fine sand (B) at a high rotational speed (1000 rpm), while the OCP value of the former was higher than that of the latter at a low rotational speed (500 rpm). This situation seems to indicate that the coarse sand (A) and medium-fine sand (B) were more aggressive at a higher and lower rotational speed, respectively. Fig. 5(b) shows the OCP values significantly decrease with the rotational speed. This scenario indicates that the erosion-corrosion of the Q235 carbon steel samples was aggravated upon increasing the sand content and rotational speed.

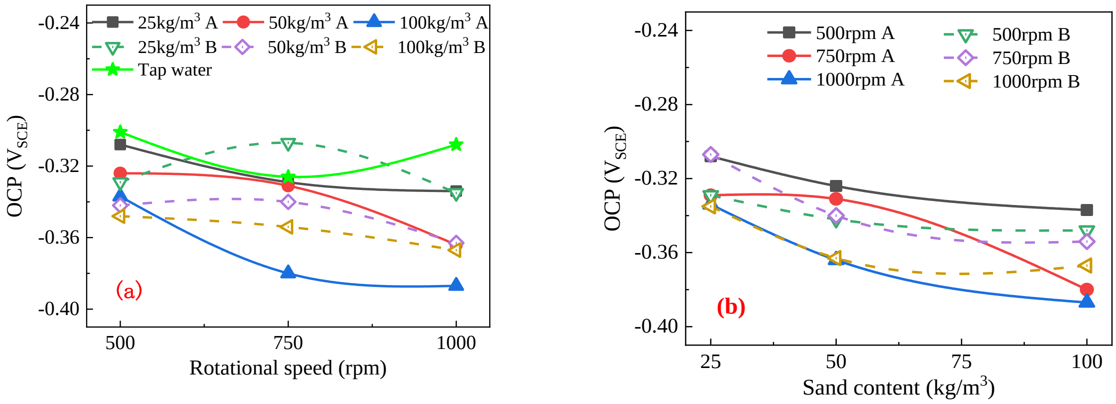

Figure 3. The OCP values of Q235 carbon steel after 8 h of the erosion-corrosion test at different (a) rotational speeds and (b) sand contents.

3.2 Electrochemical impedance spectroscopy

Fig. 4 and 5 show the EIS results of the carbon steel samples obtained under the different conditions studied. In the Nyquist plots, two obvious capacitive arcs were observed and the radius of the capacitive arcs at low frequency obviously decreases with the sand content and rotational speed. This scenario was consistent with the OCP results, suggesting the activity of the steel surface was enhanced upon the increasing sand content and rotational speed [12,13]. On the other hand, the results in Fig. 4 and 5 show that the samples in the solution containing coarse sand (A) seem to be more seriously eroded than their counterparts in the solution containing medium-fine sand (B) with the same sand content at higher rotational speed (1000 rpm).

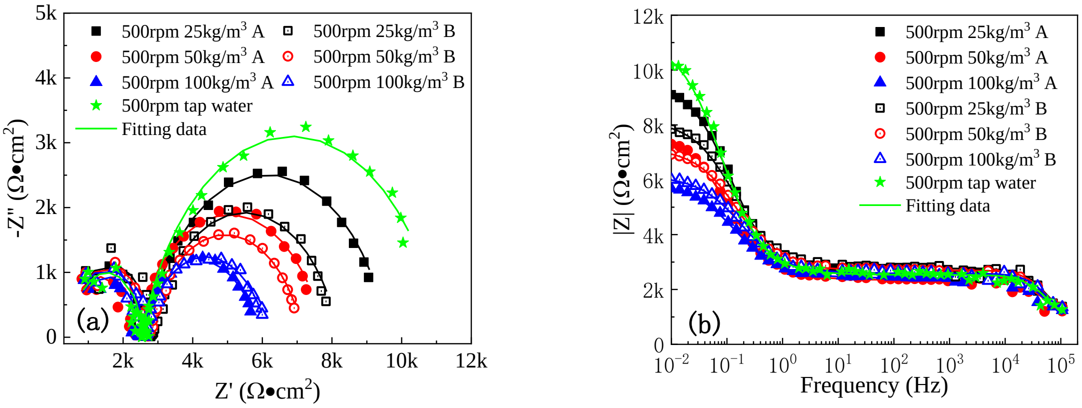

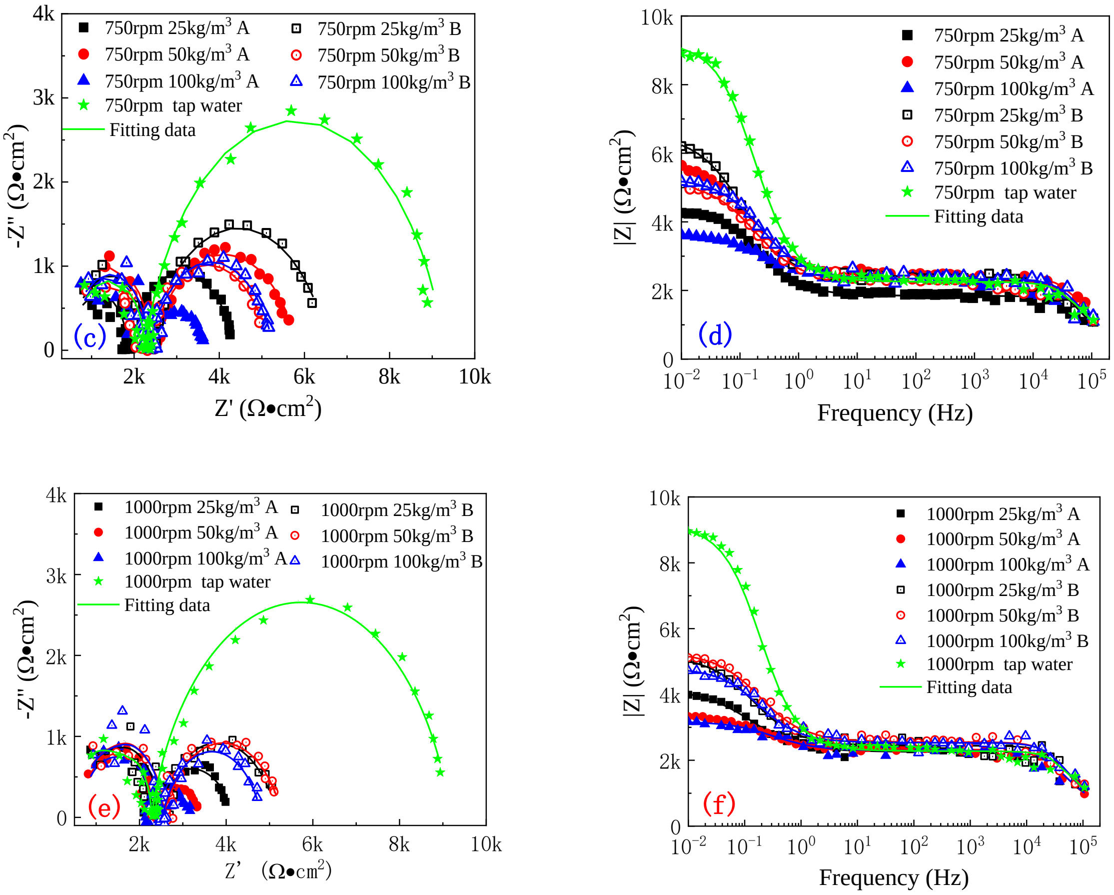

Figure 4. EIS results obtained for the Q235 carbon steel samples after 9 h of the erosion-corrosion test under different conditions: Nyquist (a) and Bode (b) plots obtained at 500 rpm; Nyquist (c) and Bode (d) plots obtained at 750 rpm; and Nyquist(e) and Bode (f) plots obtained at 1000 rpm.

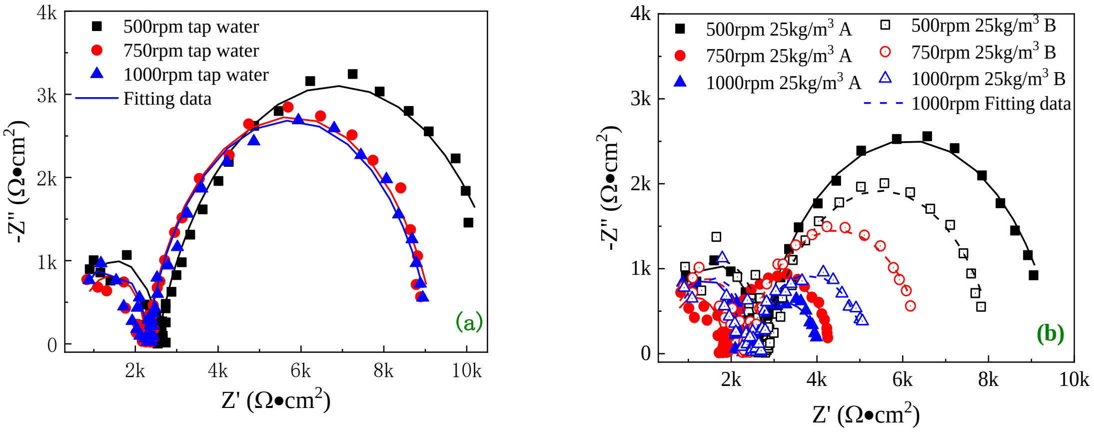

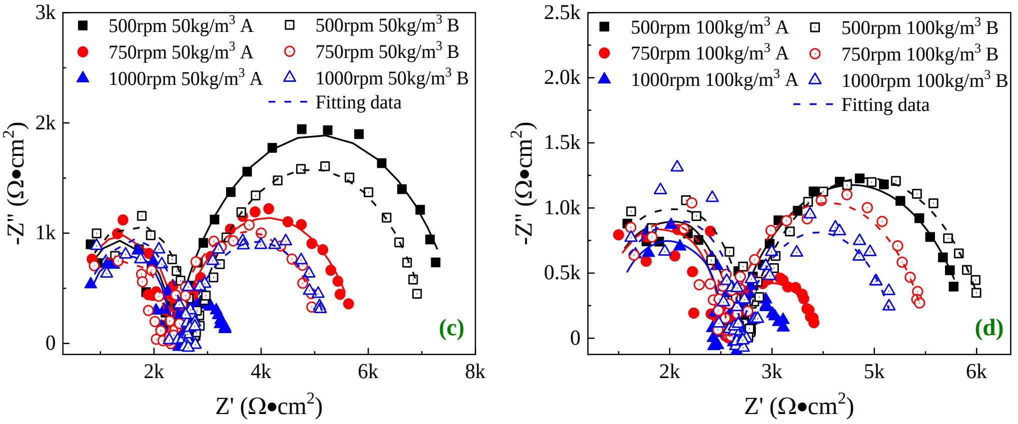

Figure 5. Nyquist plots obtained for the Q235 carbon steel samples after 9 h of the erosion-corrosion test in solutions with different sand contents: (a) without sand, (b) 25 kg/m^3, (c) 50 kg/m^3 and (d) 100 kg/m^3.

An equivalent circuit [14, 16] shown in Fig. 5 was applied to simulate the EIS results, where R_{sol} is the solution resistance, R_f and C_f are the resistance and capacitance of the rust layer on the steel surface, respectively, R_{ct} is the charge transfer resistance, and *CPE* is the constant phase angle element, used to replace the double layer capacitor *Q*.

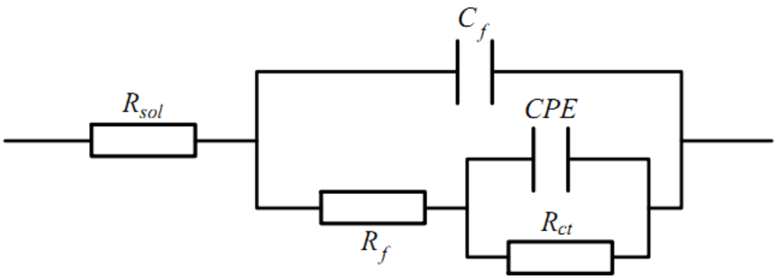

Figure 6. Equivalent circuit used to simulate the EIS results.

The fitting results of R_{ct} are presented in Fig. 7. With the exception of the value of the samples in tap water, the R_{ct} values ranged from ~1500 to 7000 Ω·cm^2 for the samples in the solution containing sand, in which the maximum R_{ct} was almost 4.5 times higher than the minimum value. In addition, the average R_{ct} value for carbon steel in the coarse sand (A) solution (2988 Ω·cm^2) was lower than those of their counterparts in the medium-fine sand (B) solution (3525 Ω·cm^2), which were significantly lower than that in tap water (7527 Ω·cm^2). When the rotational speed increases from 500 to 1000 rpm, the R_{ct} value of Q235 carbon steel in the solution containing coarse sand (A) decreases by 75.77%, while that of the steel sample in the solution containing medium-fine sand (B) only decreased by 39.98%. When the sand content increases from 25 to 100 kg/m^3, the R_{ct} value of the carbon steel samples decreased by 49.72 and 29.7% in the former and the latter solutions, respectively. The fitting results for R_{ct} further confirm that the carbon steel was more seriously eroded by increasing the sand content and rotational speed. In comparison, the solution containing coarse sand (A) was more erosive than the solution containing medium-fine sand (B) with the same sand content at higher rotational speed (1000 rpm), while the latter was more erosive at a lower rotational speed (500 rpm). This can be attributed to the total impact energy of sand on the steel surface. When the sand content and rotational speed increases or the particle size changed from coarse (A) to medium-fine (B), the surface of the carbon steel experiences a higher impact energy and the activity of the surface was enhanced during the erosion-corrosion experiment [17, 18]. As a result, the R_{ct} value of the carbon steel samples decreases with the particle size, sand content, and rotational speed. Simultaneously, coarse sand (A) was more aggressive at the higher rotational speeds, while medium-fine sand (B) was more erosive at the lower rotational speeds.

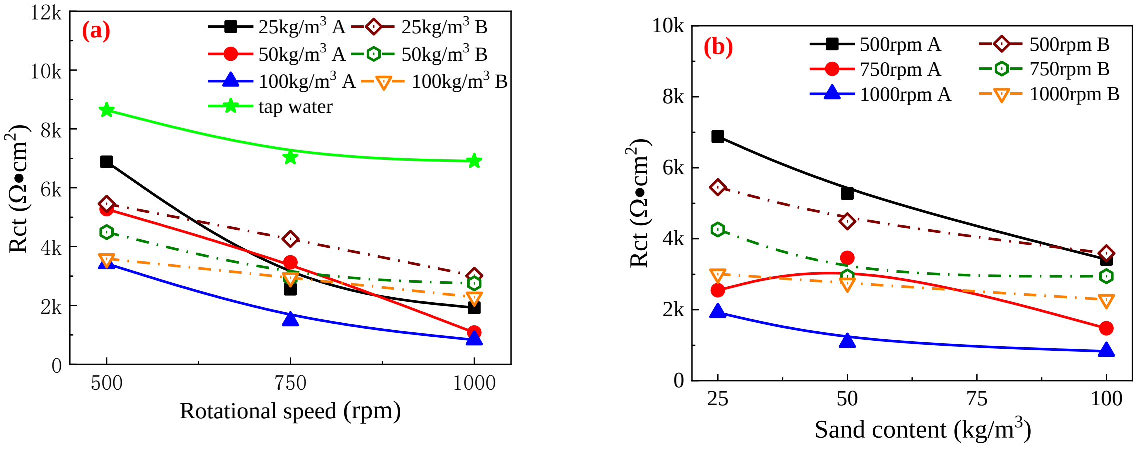

Figure 7. Fitted R_{ct} values obtained for the Q235 carbon steel samples under different conditions: (a) Rotational speed and (b) sand content.

3.3 Polarization curves

Fig. 8 shows the polarization curves obtained for the carbon steel samples in sand-containing solutions.

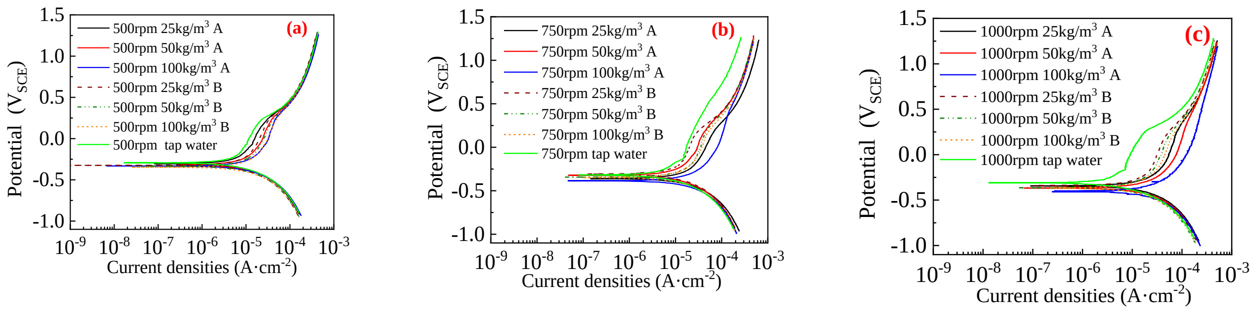

Figure 8. Polarization curves obtained for the Q235 carbon steel samples after 10 h of the erosion-corrosion test at (a) 500, (b) 750 and (c) 1000 rpm.

It is notable that the cathodic polarization curves of the carbon steels do not show any significant difference, while the anodic zones exhibit obvious differences under the various conditions studied. This phenomenon indicates that the reduction process of the erosion-corrosion behavior was charge transfer controlled on the Q235 carbon steel surface [19], which was not affected by the rotational speed and sand content. Simultaneously, no obvious passivation zones were observed in the anodic polarization curves and the anodic current densities of the Q235 carbon steel samples increase upon increasing the rotational speed and sand content. The polarization curves, together with the R_{ct} results, suggest the activity of the steel surface was improved using a higher rotational speed and sand content.

The pure erosion current densities (i_{eros}) of the carbon steels were also calculated from the polarization curves under full cathodic protection [10] and the results presented in Fig. 9. The i_{eros} value obviously increases with the rotational speed and sand content, in which the highest and lowest i_{eros} values of the Q235 carbon steel samples in the sand-containing solutions were 19.06 and 5.34 μA /cm^2, respectively. When compared to the value of several hundred μA /cm^2 observed for carbon steel subjected to erosion-corrosion in Cl-containing solutions reported in previous studies [20, 21], the i_{eros} values were much lower in the present study. Under various rotational speeds, the lowest i_{eros} value was always obtained from the carbon steel sample in tap water. When rotational speeds of 500, 750 and 1000 rpm were used, the i_{eros} values of the carbon steel samples in the solution containing coarse sand (A) were 0.91, 1.28 and1.48 times higher than their counterparts in solutions containing medium-fine sand (B). This suggests that the erosion damage of coarse sand (A) was more serious than that caused by medium-fine sand (B) at a higher rotational speed, while the erosion caused by the medium-fine sand (B) was more significant at a lower rotational speed.

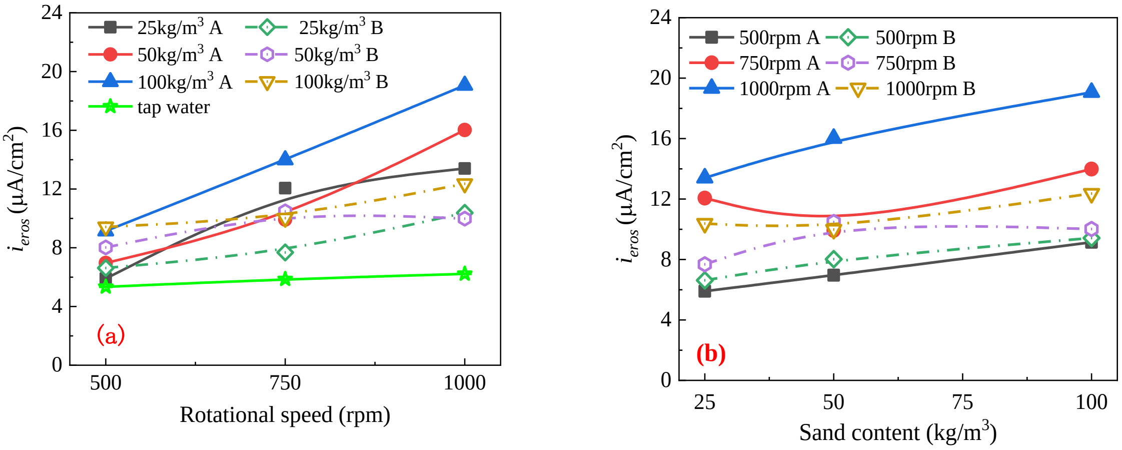

Figure 9. Pure erosion current density of Q235 carbon steel samples after 10 h of erosion-corrosion test at different (a) rotational speeds and (b) sand contents.

3.4 Erosion-corrosion behavior

The total materials loss rate (w_{total}) can be divided into weight loss rate caused by pure erosion (w_{eros}) and pure corrosion (w_{corr}), as shown in Eq (2).

$$w_{total} = w_{eros} + w_{corr} \qquad (2)$$

The total material loss rate (w_{total}) caused during the erosion-corrosion experiment was measured using the weight-loss method, according to Eq (1). The pure erosion loss rate (w_{eros}) was obtained from the polarization curve under full cathodic protection [10]. Based on Eq (3), the pure erosion loss rate (w_{eros}) can be obtained from the pure erosion current densities (i_{eros}), as follows [22, 23]:

$$w_{eros} = \frac{\mathrm{A} \times i_{eros}}{\mathrm{n} \times \mathrm{F} \times \rho} \times 87600 \qquad (3)$$

where A is the atomic weight, n is the number of electrons transferred via a chemical reaction, F is Faraday's constant, and ρ is the density of the alloy. The weight loss rate (w_{corr}) caused by pure corrosion can then be calculated for the erosion-corrosion experiment, according to Eq (2) and Eq (3).

Fig. 10 shows the results of the total materials loss rate (w_{total}), weight loss rate caused by pure erosion (w_{eros}) and weight loss rate caused by pure corrosion (w_{corr}). Fig. 11 shows the ratios of the weight loss rates caused by pure corrosion in the total weight loss rates.

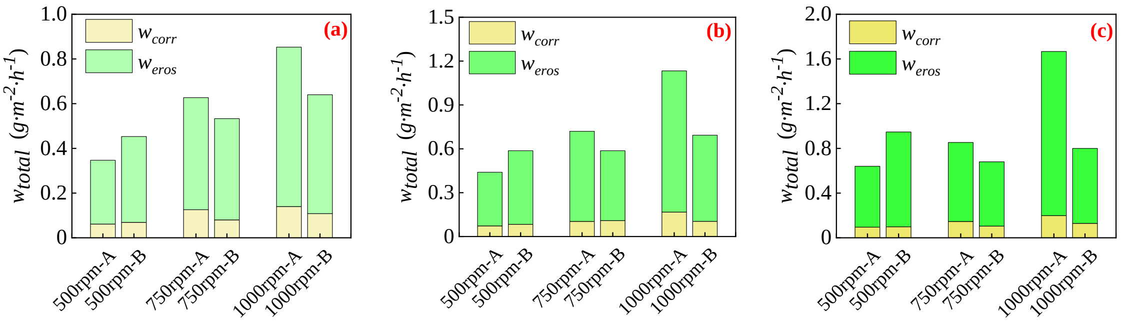

Figure 10. The total materials loss rate (w_{total}), pure erosion weight loss rate (w_{eros}) and pure corrosion weight loss (w_{corr}) during the erosion-corrosion test: (a) 25, (b) 50 and (c) 100 kg/m^3.

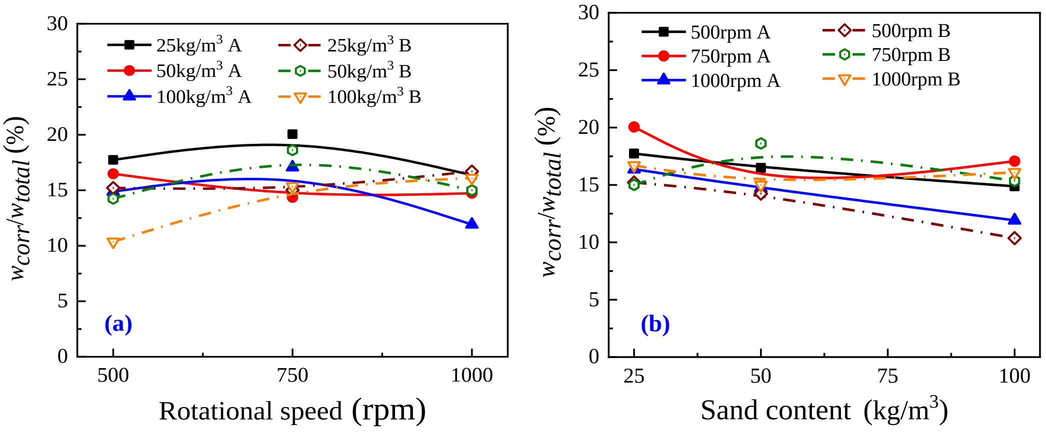

Figure 11. The ratio of weight loss rate caused by pure corrosion in the total weight loss rate under various conditions: (a) different rotational speeds and (b) different sand contents.

The average values of the total weight loss rate of the carbon steel samples in the solution containing coarse sand (A) were 0.72, 1.22, and 1.71 times higher than those of their counterparts in the medium-fine sand (B) solutions, respectively. The total weight loss rate results further confirm that the coarse sand (A) seriously erodes the carbon steel samples when compared to medium-fine sand (B) at higher rotational speeds (1000 rpm), while the latter sand is more aggressive than the former at the lower rotational speed. When the rotational speed reaches 1000 rpm, the w_{total}, w_{corr} and w_{eros} values of the carbon steel sample in the former solution were 154.60, 121.94 and 160.76% of the values of the samples in the latter solution. Simultaneously, when the sand content increases from 25 to 100kg/m^3, the total w_{total}, w_{corr} and w_{eros} of the carbon steel sample in the coarse sand (A) solution increased by 71.97, 46.03, and 79.24% at the same speed, while those in the medium-fine sand (B) solution increased by 53.88, 34.20 and 57.88%, respectively.

Fig. 12 shows, the weight losses of the carbon steel samples were mainly caused by the pure erosion of the sand particles and only ~10–20% came from the pure corrosion effect. Furthermore, as the sand content increases in the solution, the weight loss caused by the pure corrosion effect slightly decreases, in which the samples in the solution containing coarse sand (A) decreased more significantly than those in the solution containing medium-fine sand (B).

3.5 Surface characterization

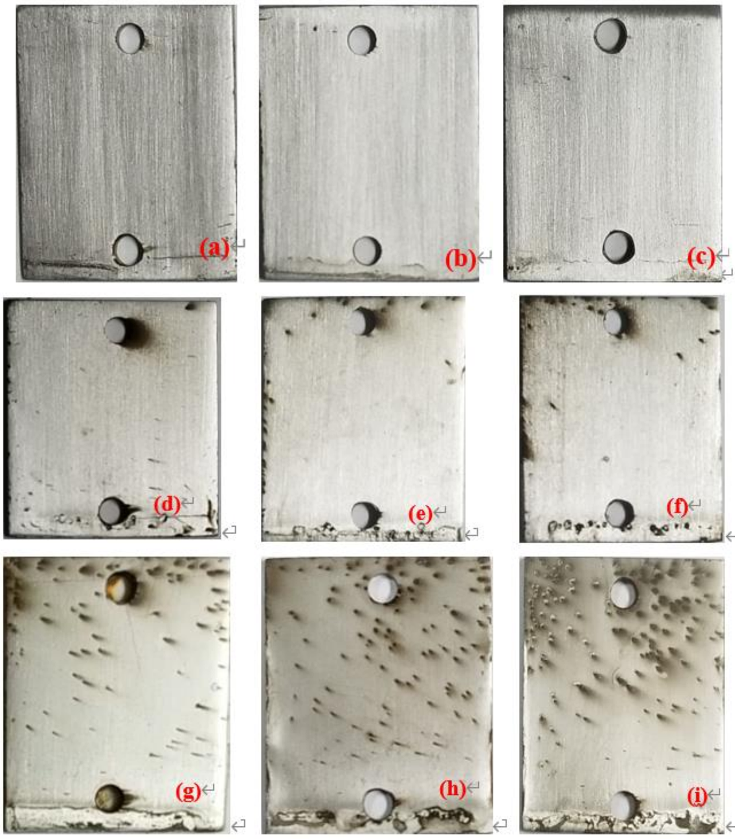

Figure 12. Photographs of the carbon steel surface after 10 h of the erosion-corrosion test under different conditions: (a) 500 rpm-tap water, (b) 750 rpm-tap water, (c) 1000 rpm-tap water, (d) 500 rpm-sand A-25 g/m^3, (e) 500 rpm-sand A-50 g/m^3, (f) 500 rpm-sand A-100 g/m^3, (g) 1000 rpm-sand A-25 g/m^3, (h) 1000 rpm-sand A-50 g/m^3 and (i) 1000 rpm-sand A-100 g/m^3.

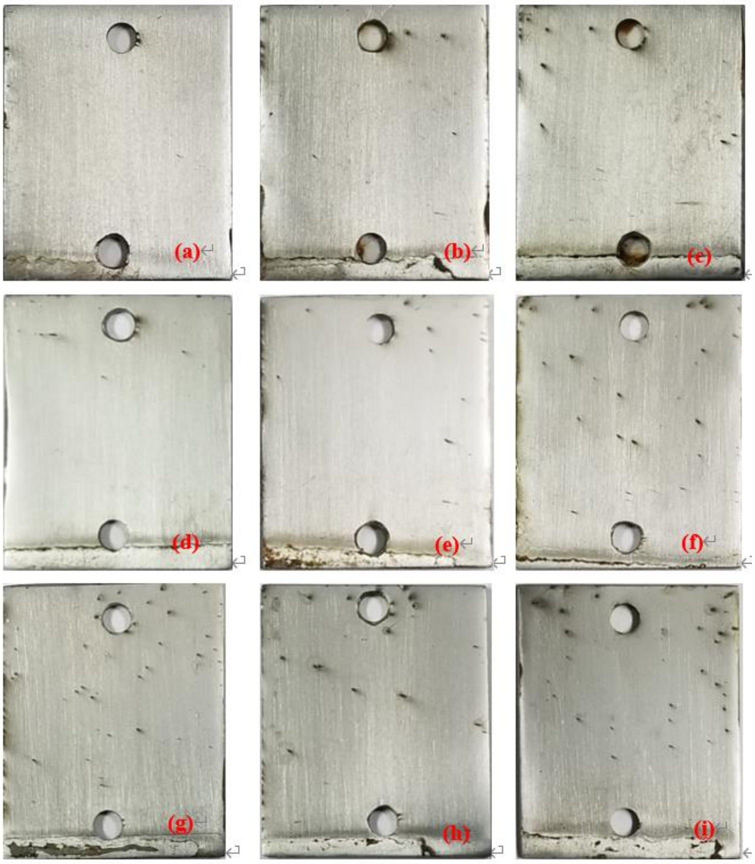

Figure 13. Photographs of the carbon steel surface after 10 h of the erosion-corrosion test under different conditions: (a) 500 rpm-sand B-25 g/m^3, (b) 750 rpm-sand B-25 g/m^3, (c) 1000 rpm-sand B-25 g/m^3, (d) 500 rpm-sand B-25 g/m^3, (e) 500 rpm-sand B-50 g/m^3, (f) 500 rpm-sand B-100 g/m^3, (g) 1000 rpm-sand B-25 g/m^3, (h)1000 rpm-sand B-50 g/m^3 and (i) 1000 rpm-sand B-100 g/m^3.

Fig. 12 and 13 display the surface states of the carbon steel samples under different conditions after 10 h of the erosion-corrosion test. It is easy to notice that the surfaces of the carbon steel samples were seriously damaged upon increasing the sand content and rotational speed, and coarse sand (A) was more aggressive than medium-fine sand (B) at the same content. This was consistent with the electrochemical results shown in Fig. 3, 7, 9 and 10.

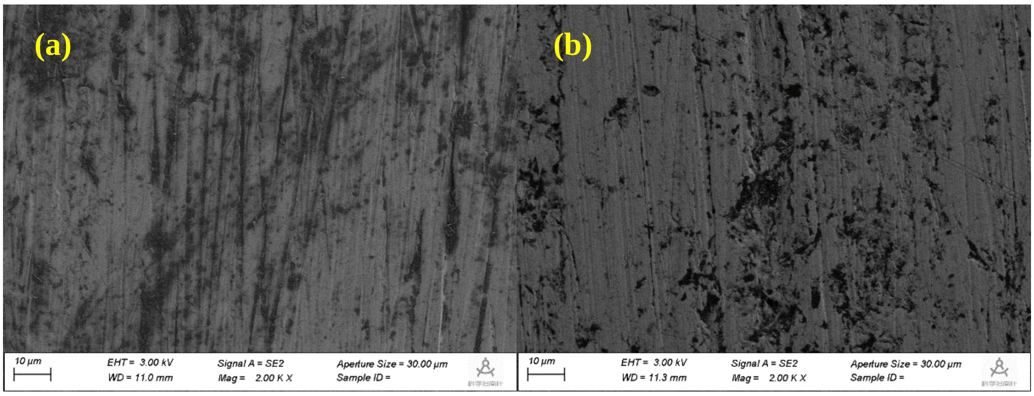

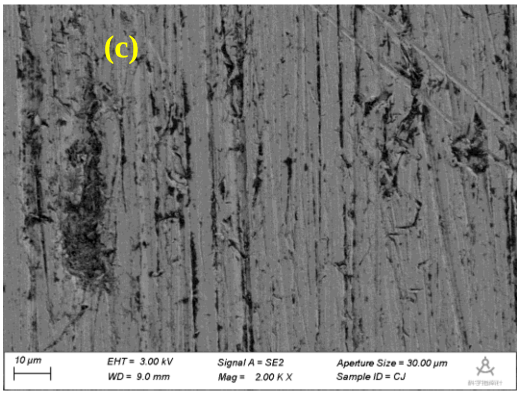

Figure 14. Morphology of the carbon steel surface after 10 h of the erosion-corrosion test in a solution with 50 kg/m^3 coarse sand (A) at different rotational speeds: (a) 500, (b) 750 and (c) 1000 rpm.

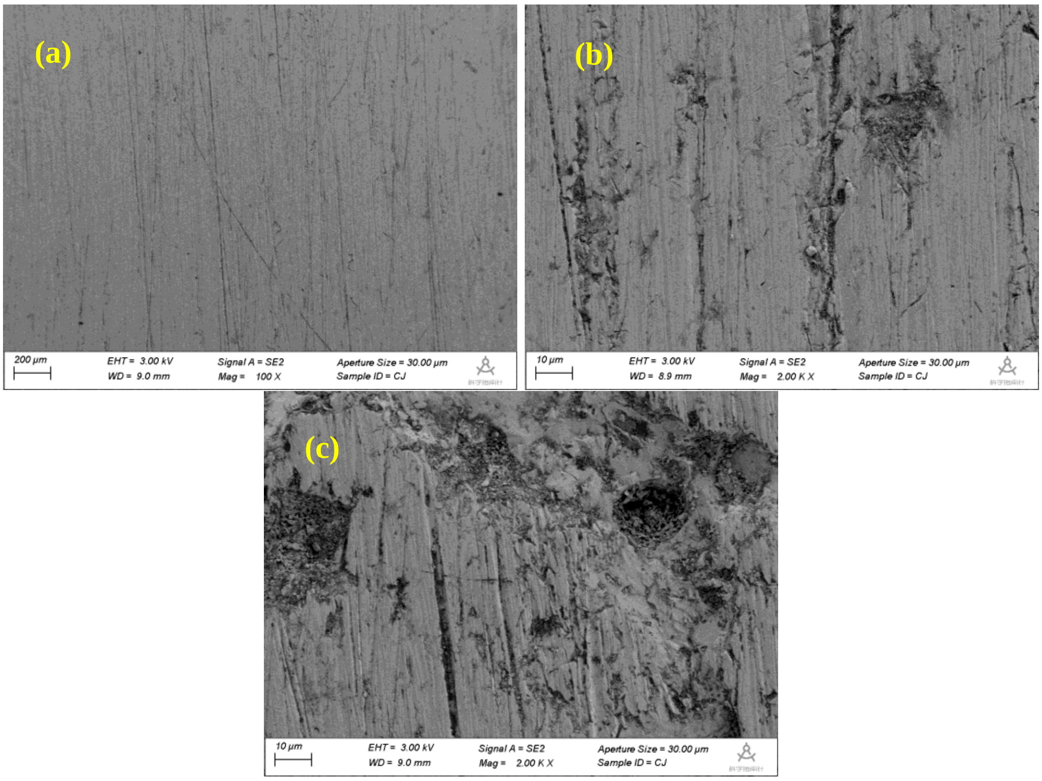

Figure 15. Morphology of the carbon steel surface after 10 h of the erosion-corrosion test in solutions with different concentration of coarse sand (A) at a rotational speed of 1000 rpm: (a) 0, (b) 25 and (c) 100 kg/m^3.

In addition, the surface morphologies of the carbon steel samples were observed using scanning electron microscopy (SEM) after 10 h of the erosion-corrosion test and the results presented in Fig. 13 and 14. In the solution containing 50 kg/m^3 coarse sand (A), the number of indentations caused by the sand particles significantly increases when the rotational speed increases from 500 to 750 rpm. When the rotational speed was further increased (1000 rpm), the indentations on the carbon steel surface became wider, which even exhibited as hollows on the surface, as shown in Fig. 14(c). Similarly, Fig. 15 shows when the sand content in the solution increases from 25 to 100 kg/m^3, the width and depth of the hollow obviously increase. This situation can be attributed to the higher frequency of the sand particles impacting on the same areas when the rotational speed or sand content of the solution increased.

4. CONCLUSIONS

The erosion-corrosion behavior of Q235 carbon steel in sand-containing solutions has been studied and the effects of the size of the sand particles, sand content, and rotational speed were investigated. The following conclusions can be drawn from the results:

(1) The weight loss rate of the carbon steel samples increased upon increasing the sand content and rotational speed in the sand-containing solutions.

(2) The solution containing the coarse sand was more aggressive than the solution containing medium-fine sand at a high rotational speed (1000 rpm), while the latter solution was more aggressive than the former solution at a low rotational speed (500 rpm).

(3) During 10 h of the erosion-corrosion test, the weight loss rate caused by the pure corrosion only accounted for 10–20% of the total weight loss rate. The weight loss rate mainly originates from the pure erosion of the sand particles.

(4) More indentations were observed on the carbon steel surface as the rotational speed and sand content increased. The indentations gradually change into hollows as the rotational speed and sand content are further increased.

ACKNOWLEDGEMENTS
The National Natural Science Foundation of China (52179061) is gratefully acknowledged.

References

1. X. Feng, Y. Tang, and Y. Zuo, *Corros. Sci.*, 53 (2011) 1304.
2. W.S. Peng, X.W. Cao, J. Hou, K. Xu, Y. Fan, and S.H. Xing, *J. Nat. Gas. Sci. Eng.*, 76 (2020) 103175.
3. X. Feng, Y. Tang, X. Zhao, and Y. Zuo, *J. Wuhan. Univ. Technol.*, 27 (2012) 994.
4. D. López, J.P. Congote, J.R. Cano, and A. Toro, and A.P. Tschiptschin, *Wear*, 259 (2005) 118.
5. P.C. Okonkwo, S. Grami, S. Murugan, and S. Khan, *J. Iron. Steel. Res., Int*. 27 (2020) 691.
6. W.J. Gou, H. Zhang, H.P. Li, F. Liu, and J.J. Lian, *Wear,* 412-413 (2018) 120.
7. Z.W. Yi, *Sichuan Water Resources*, 5(2003) 29. (in Chinese)
8. T. Wu, Y.X. Liu, J. Qin, Y. Wang, S.N. Ye, X.G. Feng, and S.L. Chen, *Int. J. Electrochem. Sci.*, 15 (2020) 8375.
9. T. Wu, J. Qin, *J. Coastal. Res.*, 95 (2020) 304.
10. B.T. Lu, J.L. Luo, *Tribol. Int.*, 183 (2015) 146.
11. J.Q. Huang, *Corrosion & Protection*, 1 (2000) 8. (in Chinese)
12. A.S. Hamdy, A.G. SaEh, and M.A. Shoei, *Electrochim. Acta*, 52 (2007) 7068.
13. X. Feng, Y. Zhao, X. Lu, V. Fattahpour, and J.L. Luo, *Corros. Rev.*, 39 (2021) 149.
14. Y.Z. Xu, L. Liu, and C.B. Xu, *J. Solid. State. Electr.*, 24 (2020) 2511.
15. X. Feng, X. Zhang, Y. Xu, R. Shi, X. Lu, L. Zhang, J. Zhang, and D. Chen, *Eng. Fail. Anal.*, 98 (2019) 49.
16. X. Feng, X. Lu, Y. Zuo, N. Zhuang, and D. Chen, *Corros. Sci.*, 103 (2016) 66.
17. H.X. Guo, B.T. Lu, and J.L. Luo, *Electrochim. Acta*. 52 (2006) 1108.
18. T. Xu, L. Zheng, K. Wang, and R. Misra, *Int. Mater. Rev.*, 58 (2013) 263.

19. Z.B. Zheng, Y.G. Zheng, W.H. Sun, and J.Q. Wang, *Corros. Sci*., 76 (2013) 337.
20. E. Mahdi, A. Rauf, and E.O. Eltai, *Corros. Sci*., 83 (2014) 48.
21. B.T. Lu, J.F. Lu, and J.L. Luo, *Corros. Sci*., 53 (2011) 1000.
22. N. Khayatan, H. M. Ghasemi, and M. Abedini, *Wear*, 380 (2017) 154.
23. ASTM Standard G 102-04, ASTM International, USA, 2004.